Optical scattering measurements and implications on thermal noise in Gravitational Wave Detectors Test-Mass Coatings

Lamar Glover[1], Michael Goff[1], Jignesh Patel[1], Innocenzo Pinto[2], Maria Principe[2], Travis Sadecki[3], R. L. Savage[3], Ethan Villarama[1], Eddy Arriaga[1], Erik Barragan[1], Riccardo DeSalvo[1,2], Eric Do[1], Cameron Fajardo[1],

[1]*California State University, Department of Physics and Astronomy, 5151 State University Drive, Los Angeles CA 90032, USA*

e-mail address: lglover3@calstatela.edu

[2]*University of Sannio at Benevento, 82100 Benevento, Italy and INFN (Sezione di Napoli), Italy*

[3] *LIGO – Hanford Observatory, Richland, WA 99352, USA*

Photographs of the LIGO Gravitational Wave detector mirrors illuminated by the standing beam were analyzed with an astronomical software tool designed to identify stars within images, which extracted hundreds of thousands of point-like scatterers uniformly distributed across the mirror surface, likely distributed through the depth of the coating layers. The sheer number of the observed scatterers implies a fundamental, thermodynamic origin during deposition or processing. These scatterers are a likely source of the mirror dissipation and thermal noise foreseen by V. Braginsky and Y. Levin, which limits the sensitivity of observatories to Gravitational Waves. This study may point the way towards the production of mirrors with reduced thermal noise and an increased detection range.

Keywords: scattering, thermal noise, dissipation, quality factor, crystallites, gravitational waves
PACS: 95.55.Sh, 93.90.+y, 13.15.+g

I. INTRODUCTION

Vladimir Braginsky[i,ii] and Yuri Levin[iii] predicted that thermal noise of coatings would limit the sensitivity of Gravitational Wave detectors. The mirror test masses of LIGO[iv,v] have been specifically designed and constructed with multilayered interference coatings[vi] via ion-beam deposition to minimize optical absorption, mirror thermal noise[vii,viii] and light scattering[ix]. As such, an ideal mirror would appear black when viewed off axis from a source of illumination. However, photographs of an Advanced LIGO End Test Mass illuminated by the 100 kW interferometer stored beam taken at a 9.8° angle of the stored beam show a large number of light scattering points. The images are similar in appearance to star clusters (Figure 1). Therefore they were analyzed with DAOPHOT[x], an astronomical software tool developed by the National Optical Astronomy Observatory[xi] to identify stars within galaxies. Initially, it was assumed that the scattering was caused by dirt, which DAOPHOT ignored as nebulae. It identified hundred of thousands of diffraction-limited, weak light scatterers, many per mm^2. The unexpectedly large number, and uniform dispersal of these scatterers is not compatible with dirt. Actual scatterers must be sub-micron is size to produce large-angle scattering. Their brightness distribution suggests that they may also be uniformly distributed in depth within all the coating layers.

Since the overall absorption, measured by the mirror heating, is less than ¼ ppm, the relatively larger scattering must be a result of minuscule refraction index fluctuations that do not absorb energy. These density fluctuations are due to either denser proto-crystal formations or small, localized density deficits (voids).

The uniform distribution also implies that the scatterer generation during the deposition process itself is likely of a thermodynamic or statistical nature. While defects are observed in deposited glasses, it is important to note that molten glasses, such as the fused silica mirror substrate of the mirrors, are free of this kind of scatterers.

Ion beam deposited glass layers have been shown to have low quality factors, in the thousands, or tens of thousands, as compared with the many millions, or even billions, measured in high quality molten glasses. The mechanical losses associated with the lower quality factor of the coatings cause excess thermal noise in the mirror that, in its turn, limits the sensitivity to and detection range of gravitational wave events. Thus far, there has been no clear identification of the source of the excess dissipation in coating layers. It will be shown here that the observed scatterers are the likely locus of the larger than expected coatings mechanical losses. While the exact nature of the light scatterers cannot be identified at this time, their observation may become an important diagnostic tool to develop deposition procedures that mitigate optical scattering as well as thermal noise.

A more detailed analysis will be presented in a companion paper[xii].

II. METHODS AND PROCEDURE

Using DAOPHOT, a large number of tiny scatterers, diffraction limited irregularities in light reflection, have been detected within the mirror coating layers. The search tool is optimized to detect point-like objects, ignoring "nebula-like" dirt particles, which locally masked the underlying scatterers (see figures 1 and 4). The camera lens cannot resolve the points identified by DAOPHOT, which are visible as, and are identified by their congruence with, Airy disk profiles generated by the camera lens aperture. Best fit procedure extracts the position (in the X,Y plane) and amplitude information of each candidate. DAOPHOT identified the positions and relative luminosity of the scatterers in 40 images of varying exposure times that were acquired at the LIGO Hanford observatory in November 2015, when the interferometer was running at about 100 kW of stored power in its Fabry-Perot arm cavities.

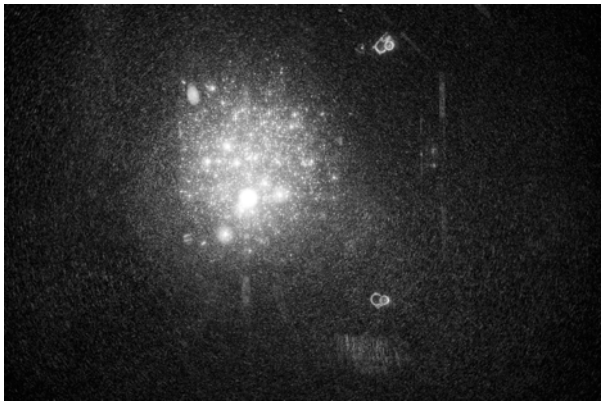

Figure 1. *Photograph of an End Test Mass; Exposure time of 1.3 seconds. Light blobs are interpreted as surface dirt. The rings and faint straight lines on the right side of the image are part of the mirror support structure.*

There is a varying degree in scatterer quality within the images, which can be attributed to either pixel saturation or scatterer crowding. The scatterer Airy disk size on the CCD corresponds to ~80μm wide spots on the mirror surface. The crowding observed in high exposure images is due to the size of the Airy disks. The actual scatterers must be sub-micron in size to generate large angle scatter, thus they are actually widely separated within the coating layers of the coating.

It is observed that the shapes of Airy disks at larger exposure times are amplitude-dependent, due to CCD saturation. The effects of saturation are illustrated in Figure 2.

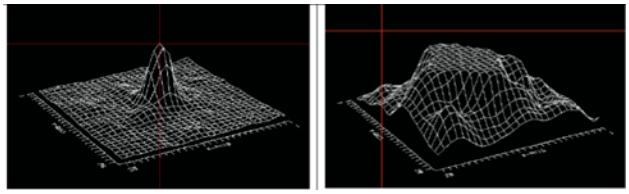

Figure. 2. *Contour Plot of a non-saturated Detected Scatterer (left) and of an oversaturated one (right). The latter are found with increasing frequency amongst images with longer exposure time.*

The 40 images analyzed varied in exposure times from 1.25×10^{-4} to 1.3 seconds. The numbers of detected scatterers per image were graphed as a function of their respective exposure times in figure 3. The growth of the number of detected points is nearly linear, with a saturation occurring above 0.2 s exposure, which was attributed, by manual observation, to crowding of saturated airy disks rather than an actual cutoff of weaker scatterers. It appears that a population of apparently even weaker scatterers, progressively less illuminated in deeper and deeper mirror layers, lies behind the detected ones.

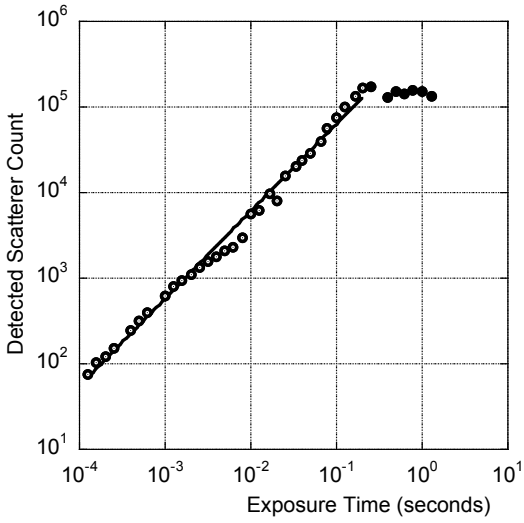

Figure. 3. Detected number of scatterers vs. exposure time: the line is a fit performed with a power law a x^b on the points with a white center. The fit gives an exponent b=1.02, compatible with slope ~1, until saturation occurs.

III. METHOD LIMITATIONS

Shorter camera exposure times result in less saturated and smaller Airy disk shapes, but also in a smaller number of scatterers detected, with the less luminous ones fading into the CCD image "dark" pixel count. Longer exposure times proved to be problematic due to the fact that when the CCD saturation count of 255 is exceeded, there seems to be outflow of the excess charge on the neighboring pixels, as illustrated in figure 2. To mitigate these shortcomings, it is intended to use sequences of images taken in rapid

succession at the same shortened exposure times once more images are available. It is expected that adding the pixel counts of these photos after proper re-centering, to compensate for apparatus movements, and using the camera in "raw data" mode, with 14 bit resolution will generate images with much higher-dynamic range that will reveal the weaker scatterers without oversaturating the bright ones. A more efficient subtraction of scatterers may be expected from DAOPHOT and a number of fainter scatterers may become visible, thus producing a more reliable luminosity distribution curve. At the time this work was written, the two observatories were offline for service upgrades. This work was therefore limited to the best available images.

It should be noted that these scatterers have been observed previously[xiii,xiv]. At that time, it was surmised that the scatterers were laser speckle, which is unlikely because the speckle pattern is observed to remain stable, even for beam movements over the mirror surface, and speckle patterns do not mimic well the Airy disk patterns that were observed. Interestingly, previous scattered light measurements performed from the same viewports on the initial LIGO mirrors (Fig. 3 of reference XII) found scattered intensity levels in excess of what had been estimated using the known mirror substrate roughness. The scatterers studied here may account for some of that excess power.

It should also be noted that DAOPHOT was already used in angular dependence studies of scattering on sample mirrors[xii], similarly finding multiple scatterers throughout the captured images. Angular power information cannot be produced in the measurements described here because all the images were taken from a single location.

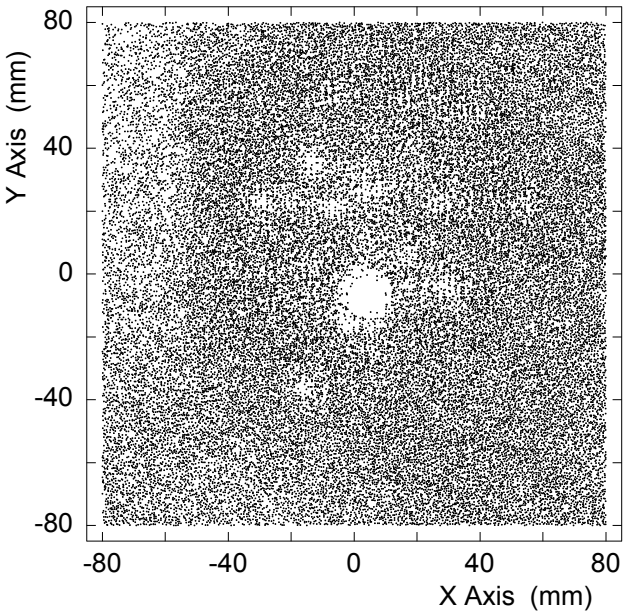

Figure. 4. DAOPHOT-detected scatterers with 0.763 second exposure. Smear due to dirt limits "DAOPHOT's" detection efficiency in some areas. The density of detected scatterers is lower on the beam spot tails, due to the rapidly decreasing illumination, but it is otherwise compatible with a constant value.

It is worth mentioning that DAOPHOT produces scatterer positioning with a micron-level precision. Thus monitoring the scatterers' apparent motion over time provides a tool to accurately measure the transversal motion of mirrors in the interferometers. Similarly, monitoring the apparent changes of scatterer luminosity on the two sides of a beam spot provides a tool to measure the transversal beam motion with respect to the mirror surface. Both informations are not currently available at this precision level.

Development of these tools, as well as more details on the technique used, are discussed in a companion paper[xii].

IV. RESULTS

The photographs were taken with approximately 100 kW of 1064 nm wavelength stored beam illuminating the test masses. The camera utilized a 240mm lens, set at f/11 and ISO 100 with exposure times varying between 1.25×10^{-4} to 1.3 seconds.

The pixel size corresponds to ~80 μm on the mirror surface in both the X and Y directions. It was calibrated using the straight edges of the mirror support structure, visible on the right side of figure 1. The scatterer distribution in figure 4 is clearly not uniform, which can be attributed to areas where dirt inhibits DAOPHOT's identification process. This is visible as patches with strong deficit of scatterers.

The illumination level affects the number of detected scatterers, according to the slope fit in figure 3, with their number decreasing on the wings of the stored beam profile. It is clear that the average density of scatterer/mm^2 obtained by dividing the number of points by the field of view area is merely a lower limit.

The distribution of the identified scatterers was studied in a cropped section of an image containing the core of the stored beam, taken at 0.763 s exposure.

The following procedure was implemented to produce an evaluation of the actual scatterers' density if the illumination was uniform and the dirt absent.

The cell region of interest was first sub-divided into a 10 by 10 matrix of cells, each 2.56 cm^2 in size. The detected scatterers were counted in each of the 100 cells. The scatterer's count varied from 250 to 1070 counts/cm^2, with a mean of 650 and a standard deviation of 210 counts/cm^2. The standard deviation is an order of magnitude larger than the ±16 counts/cm^2 that could be expected by statistical fluctuations, reflecting the masking effects of dirt, and the changing illumination level.

Given the fact that dirt masks out detected scatterers, and that the beam profile reduces the number of detected scatterers in the wings, the largest value in the 100 cells is considered to be the best estimator of the undisturbed scatterer density, i.e. the actual scatterer density is at least 64% higher than the gross average estimation of 1658 scatterers per bin. It remains to be established if the highest cell count is representative, i.e. if it is unaffected by dirt. In absence of dirt, the scatterers' distribution should be uniform, if the distribution of scatterers in the bin cell with the highest count is uniform, it is probable that the scatterer count in that cell is unaffected by dirt.

Rows / Columns	1	2	3	4	5	Max.	133
1	99	123	99	109	109	Sum	2724
2	99	110	119	103	105	Points	25
3	108	103	105	115	109	Mean	109
4	106	108	133	108	115	Std Dev.	8.5
5	104	104	105	124	102	Std Error	1.7

Table 1: number of scatterers detected by DAOPHOT in the 10.2 mm^2 subdivisions of highest count cell. The last two columns list the statistical analysis of the panel data. The standard deviation of 8.5 counts is in good agreement with the expected statistical fluctuation √109=10.4, indicating that dirt is likely absent in this cell, and the scatterer distribution is uniform.

The highest count cell is close to the beam center. It was subdivided into another 5 x 5 matrix of cells and their content counted. The results are reported in figure 5 and table 1. The data in table 1 is in agreement, within statistical error bars, with the Gaussian predicted by a uniform distribution of scatterers of average 109 counts. illustrating the uniform distribution of the scatterers in cell 6,6. It is therefore concluded that, excluding the points where the image smears due to dirt, the scatterer density around the beam center, at the exposure level of figure 4, was approximately 10.7/mm^2.

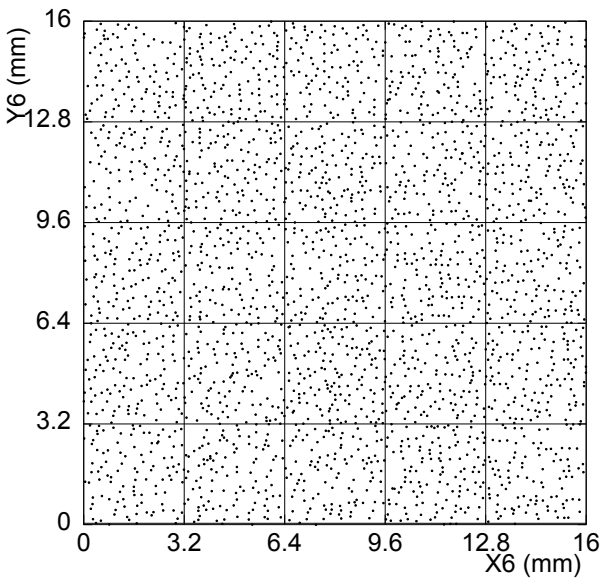

***Figure 5**: scatter plot of the detected scatterers of highest count cell.*

The amplitude distribution of the events detected by DAOPHOT in the image of 0.763 second exposure is shown in figure 6. It is important to note that coating layers near the surface are much more strongly illuminated than deeper layers. Only the scatterers from shallow layers are visible. To make an evaluation of the overall number of scatterers actually present throughout the mirror, one should take into consideration the illumination drop with the coating layer number.

In addition, because the camera observation angle from the beam axis is small (9.8°), the backscattered light from deeper layers is reduced by approximately the same factor as the illumination. The two effects amount to a strong exponential attenuation, resulting in the scatterers from the second layer being visible with 25% of luminosity and 6.3% from the third layer[xv]. In practice, assuming that the scatterers are concentrated in the Tantala layers, only scatterers present in the top layers contribute to figure 4 and 5 while scattering from deeper layers is hardly visible. Because there are 26 layers in a coating, about an order of magnitude of additional scatterers can be expected to exist undetected below the surface, i.e. hundreds per square millimeter.

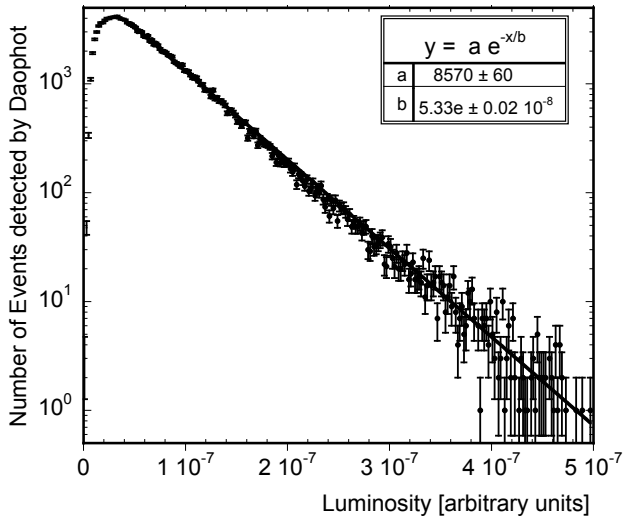

Figure 6: Detected scatterer luminosity distribution the exponential decay fit is performed only on the points above $Z=0.5\ 10^{-7}$. The cutoff at low amplitude is due to the dark pixel count level of the CCD.

V. IMPLICATIONS IN DISSIPATION AND THERMAL NOISES

It is very unlikely that such a high and uniform scatterer density can be accidental. It requires a fundamental origin, probably in the deposition process.

Large angle scatter without absorption requires fluctuations of refraction index at sub-wavelength scale. As the chemical composition of the material is uniform, density fluctuations are necessary. Fluctuations of either sign are possible.

Positive refraction index fluctuations are given by crystallites, which are fluctuations with higher molecular order and larger density. Previous studies have shown evidence of large mechanical losses within the coating layer material.[xvi] There, materials are observed to evolve into crystal (columnar) growth in thicker film depositions of the same materials, as well as in films that have undergone annealing, which imply the presence of crystallite seeds.[xvii,xviii] The crystallites have a minimum critical size, due to the competition between the high energetic cost of the dangling and frustrated bonds on the surface and the energy gain of crystallization, which is proportional to the volume. Crystallites that are too small tend to dissolve back in the glass during annealing, while larger ones tend to grow. Crystallites can be depressed by alloying different materials, which historically was done to improve coating performance even before this reasoning was developed[vi], or by nano-layering within each coating layer[vii, xviii].

Negative refraction index fluctuations are due to local density deficit in the glass. Glasses are always less dense than their crystalline counterpart, due to a statistically uniform distribution of atomic-size voids, but evaporation-deposited glasses are even less dense and can present larger deviations from uniformity. The coating glass appears optically uniform, but one can expect scattering of light from lower density volumes if the void size distribution has sufficiently large fluctuations, and/or if a sufficient concentration of atomic-size voids happens in the scale of a fraction of a wavelength. The ensuing local refraction index deficit could then produce the observed scattering. It is suggested that low-density fluctuations may be mitigated by means of hot substrate deposition, ion-assisted deposition, annealing or other production techniques.[xix ,xx]

While it is impossible to distinguish between high- and low-density fluctuations with the observational methods used here, both lower and higher density zones are expected to have a larger amount of loose or dangling bonds than the rest of the glass. Both cases can be conceptualized as two-level systems represented by asymmetric double-well potentials in some configuration coordinate. The distribution of corresponding double-wells in the atomic displacement depends on the distribution of bond angles and frustrated bonds in the amorphous material[xxi]. As an oversimplified picture, one could imagine an atom "flopping" from one side of a bond to the other during stress propagation, thus absorbing energy and dissipating it in the thermal bath. It is clear that these defects can exist on different length and energy scales, ranging from local, atomic-sized defects such as dangling bonds to larger scale effects such as those that produce two level systems.

The observational method does not allow distinguishing between these two possibilities. Even if one cannot ascertain the exact cause of the fluctuations, they are equally likely sources of the excess of mechanical losses in evaporated glasses. When considering that thermal noise is one of the major sources of noise in gravitational wave detection, the identification of its source has major implications in regards to the optimization of production procedures and ultimately improved reach of the apparatus.[xxii]

VII. CONCLUSIONS

The analysis presented here has shown that, when the LIGO test masses are exposed to the high intensity light of the interferometer stored beam, a large and unexpected number of optical scatterers is detected within the mirror coating layers.

Theoretical material science considerations indicate that these scatterers are either nucleation centers, density voids, or a combination of the two, and a likely locus of the anomalous dissipation in the mirror coatings and source of its thermal noise. Observation of these previously overlooked scatterers may point the way towards a mitigation strategy.

The methods developed here will also allow tracking the motion of the mirrors and the beams on the mirrors, important diagnostic and feedback tools for the observatories. The feasibility of these tools is discussed in

a technical companion paper.

The background of the detectors could be reduced if some of the glitches found in the gravitational wave signal channel were to correlate with the motions that can be detected with the methods proposed here.

Reduction of thermal noise, reduction of scattering, better alignment, and reduction of glitches are all elements that can potentially increase the detection range of LIGO.

The methods proposed do not give depth information for the scatterers. It is important to precisely and systematically locate the scatterers within the mirror coating thickness, which can perhaps be done with microscope observations.

VIII. ACKNOWLEDGEMENTS

The authors gratefully acknowledge Mara Salvato for suggesting the use of DAOPHOT, without which this work would have been impossible. The authors would like to also thank Hiro Yamamoto for his useful comments. Most of the work was performed by undergraduate students as part of the PHYS-470 advanced lab, supervised by LG in the framework of his master's thesis. The photos were provided by LIGO, which was constructed with funding from the National Science Foundation and operates under Cooperative Agreement No. PHY-0757058. Advanced LIGO was built under Grant No. PHY-0823459. RDS would like to acknowledge that his studies on thermal noise started from discussions and work with Yuri Levin, and later with Vladimir Braginsky. This paper has LIGO Document Number LIGO-P1600345.

[i] Braginsky, V. B., V. P. Mitrofanov, and K. V. Tokmakov. "Energy dissipation in the pendulum mode of the test mass suspension of a gravitational wave antenna." *Physics Letters A* 218.3 (1996): 164-166

[ii] V.B. Braginsky, S.P. Vyatchanin, "Corner reflectors and quantum-non-demolition measurements in gravitational wave antennae." *Physics Letters A* V. 324, 5-6 (2004) 345-360.

[iii] Levin, Yu. "Internal thermal noise in the LIGO test masses: A direct approach." *Physical Review D* 57.2 (1998): 659.

[iv] Aasi, Junaid, et al. "Advanced LIGO." *Classical and Quantum Gravity* 32.7 (2015): 074001.

[v] Abbott, B. P., et al. "GW151226: Observation of gravitational waves from a 22-solar-mass binary black hole coalescence." *Physical Review Letters* 116.24 (2016): 241103.

[vi] Harry, Gregory, Timothy P. Bodiya, and Riccardo DeSalvo, eds. *Optical coatings and thermal noise in precision measurement*. Cambridge University Press, 2012.

[vii] Villar, Akira E., et al. "Measurement of thermal noise in multilayer coatings with optimized layer thickness." *Physical Review D* 81.12 (2010): 122001.

[viii] M. Principe, "Reflective Coating Optimization for Interferometric Detectors of Gravitational Waves," *Optics Express*. 23.**9** (2015) 10938-10956.

[ix] Harry, Gregory M., and LIGO Scientific Collaboration. "Advanced LIGO: the next generation of gravitational wave detectors." *Classical and Quantum Gravity* 27.8 (2010): 084006.

[x] Peter B. Stetson, "DAOPHOT: A Computer Program for Crowded-Field Stellar Photometry." *The Astronomical Society of the Pacific*, 99.613 (1987): 191-222

[xi] National Optical Astronomy Observatory (950 N Cherry Ave, Tucson, AZ 85719), https://www.noao.edu/

[xii] Glover, Lamar, et al. "Observation of a Large Population of Optical Scatterers in the Advanced LIGO mirrors", LIGO-P1600325, (2016) submitted for publication in the Journal of Optical Society of America

[xiii] William Kells et al., "Scattered Light Loss from LIGO Arm Cavity Mirrors", LIGO Scientific Collaborative Database, LIGO-T0900128 (2009)

[xiv] Joshua Hacker, "Distinguishing Points from Glow in Scattering Images", LIGO Scientific Collaborative Database, LIGO-G1500772 (2015)

[xv] Orfanidis, Sophocles J. *Electromagnetic waves and antennas*. Rutgers University, 2002.

[xvi] Penn, S.D et al. "Mechanical loss in tantala/silica dielectric mirror coatings." *Class. Quantum Grav*. 20.13 (2003)

[xvii] Huang-Wei Pan, Shun-Jin Wang, Ling-Chi Kuo, Shiuh Chao, Maria Principe, Innocenzo M. Pinto, and Riccardo DeSalvo, "Thickness-dependent crystallization on thermal anneal for titania/silica nm-layer composites deposited by ion beam sputter method." Optics Express, 22.24 (2014): 29847-29854

[xviii] Anders, André. "A structure zone diagram including plasma-based deposition and ion etching." *Thin Solid Films* 518.15 (2010): 4087-4090.

[xix] Queen, D. R., et al. "Two-level systems in evaporated amorphous silicon." *Journal of Non-Crystalline Solids* 426 (2015): 19-24.

[xx] Queen, D. R., et al. "Excess specific heat in evaporated amorphous silicon." *Physical review letters* 110.13 (2013): 135901.

[xxi] M.D. Ediger, "Vapor-deposited glasses provide clearer view of two-level systems," *Proc. Natl. Acad. Sci. U.S.A.* 111.31 (2014): 11232.

[xxii] Pitkin, M.; Reid, S.; Rowan, S.; Hough, J. Gravitational Wave Detection by Interferometry (Ground and Space). *Living Rev. Relativity (*2011**),** 14.5